applied sciences

MDPI

*Article*

# Enhancing Detection Performance of the Phase-Sensitive OTDR Based Distributed Vibration Sensor Using Weighted Singular Value Decomposition

**Khurram Naeem [1], Bok Hyeon Kim [1,*], Dong-Jin Yoon [2] and Il-Bum Kwon [2,*]**

[1] Advanced Photonics Research Institute (APRI), Gwangju Institute of Science and Technology (GIST), Buk-gu, Gwangju 61005, Korea; knaeem@gist.ac.kr
[2] Safety Measurement Institute, Korea Research Institute of Standards and Science (KRISS), Yuseong-gu, Daejeon 34113, Korea; djyoon@kriss.re.kr
* Correspondence: bhkim@gist.ac.kr (B.H.K.); ibkwon@kriss.re.kr (I.-B.K.)

**Abstract:** We propose a weighted singular value decomposition (WSVD) to reduce the random noise in the Rayleigh backscattering signal of the phase-sensitive optical time domain reflectometry (Φ-OTDR) to enhance the detection performance of the distributed vibration sensing. A 2D image is formed by assembling the raw Rayleigh backscattering traces into a matrix form, and slowly varying fluctuation and random noise can be removed using the WSVD. Consequently, the location information and the frequency of vibration induced by the external vibration event can be extracted. A vibration event with 9 m spatial resolution is detected along a 2.4 km single mode fiber. The signal-to-noise ratio (SNR) of location information for the 102 Hz physical vibration and the 525 Hz acoustic vibration was found to be 10.7 and 12.2 dB, respectively. The SNR of the vibration events demonstrate an increase of 6–7 dB compared to the conventional method, showing the excellent denoising capability of this new approach.

**Keywords:** phase-sensitive OTDR (optical time domain reflectometry); singular value decomposition; distributed vibration sensing; structural health monitoring



**Citation:** Naeem, K.; Kim, B.H.; Yoon, D.-J.; Kwon, I.-B. Enhancing Detection Performance of the Phase-Sensitive OTDR Based Distributed Vibration Sensor Using Weighted Singular Value Decomposition. *Appl. Sci.* **2021**, *11*, 1928. https://doi.org/10.3390/app11041928

Academic Editor: Raffaele Zinno

Received: 4 January 2021
Accepted: 17 February 2021
Published: 22 February 2021



## 1. Introduction

Distributed fiber optic vibration sensors have gained much attention over the years due to their unique advantages: they are immune to electromagnetic interference, have high detection sensitivity and fast detection response, and can be deployed in harsh conditions at low cost [1,2]. For distributed vibration sensing based on optical fiber, one particular technique is the use of the phase-sensitive optical time-domain reflectometer (Φ-OTDR) [3–6]. It is attractive because it offers high spatial resolution, broad frequency range, real-time measurement, and a long sensing distance [7–9]. It can be applied to detect multiple environmental events over long distances, such as pipeline leakages, intrusion detection, perimeter security, acoustic waves, seismic activity, other structural health monitoring applications, etc. [10–13]. In the Φ-OTDR, highly coherent light pulses are launched into a sensing fiber, and the signal traces, which result from the coherent interference of Rayleigh backscattering light originating from multiple scattering centers within the pulse duration, are acquired all along the length of the sensing fiber [12]. In the event of dynamic perturbation such as vibration or intrusion at specific positions along the optical fiber, the amplitude of the backscattering signal modulates in time due to modulation of the length and refractive index profile of the fiber, which leads to localized detection of the event. However, the Rayleigh backscattering (RBS) reflections that make the signal trace of the Φ-OTDR are usually very weak, and are accompanied by random noises, such as background and environmental noise, and the noises from the optoelectronic components (e.g., phase noise from the laser source, shot noise from the photodetector) [6]. If the

pulse power is set too high to obtain a strong backscattering signal, position-dependent signal fading would be induced [14]. For these many reasons, it is quite difficult to detect the vibration events due to their relatively small signal-to-noise ratio (SNR), which not only limits the performance of the Φ-OTDR-based distributed vibration sensor in real-life applications, but also leads to frequent false alarms.

To eliminate the random noise from the backscattering signal of the Φ-OTDR and to accurately extract and improve the SNR of the dynamic events, much research has been performed. Two approaches have been mainly used. In the first approach, light amplifications are performed using the distributed Brillouin [15], the distributed Raman [16], and the hybrid scheme [17]. Although these schemes can certainly improve the SNR of the vibration event and increase the sensing range of the Φ-OTDR, they also add to the complexity and cost of the sensing system. The second approach, due to Φ-OTDR being a distributed sensor that produces raw backscattering data in large amounts, relies on the signal processing of the raw data using efficient mathematical algorithms to improve the SNR of the vibration event. More significantly, these signal-processing algorithms enhance the SNR of the event without adding any further optoelectronic components, and therefore greatly simplify the architecture of the sensing system. Several signal-processing algorithms have been demonstrated. Juarez et al. [12] demonstrated a distributed fiber intrusion sensor using Φ-OTDR based on direct detection that uses a simple averaging method to obtain the location information of intrusion detection with low SNR. Lu et al. [6] proposed a moving average and differential method for a distributed fiber vibration sensor based on coherent detection to obtain both the location information and the frequency measurement. The SNR of the location information has considerably increased by the use of the moving average and differential method. However, the averaging methods have a major drawback: they significantly reduce the bandwidth of the frequency measurement [6].

To date, various post-processing algorithms have been introduced to increase the performance of distributed vibration sensors. These algorithms are designed to process one- and two-dimensional datasets, for instance, integrated principal component analysis [18], curvelet denoising [19], empirical mode decomposition [20], fast wavelet transform [21], CEEMDAN technique [22], power spectrum analysis [23], two-dimensional edge detection [24], and two-dimensional adaptive bilateral and filtering [25].

In this paper, a novel noise-reduction technique is proposed to enhance the SNR of the distributed vibration sensor using weighted singular value decomposition (WSVD). WSVD removes low-frequency amplitude fluctuation and other random noises from the two-dimensional image matrix made by the number of raw signal-traces encoded with time- and spatial-domain information. The technique shows great potential in retrieving the location information and frequency of the vibration event precisely under the condition of strong background noise.

## 2. Theory of Weighted Singular Value Decomposition

Singular value decomposition (SVD) is a renowned and stable mathematical technique for data denoising as well as compression in the fields of imaging [26]. It has been effectively demonstrated for data reconstruction [27] and denoising [28] applications of the magnetic resonance imaging (MRI).

SVD [29] decomposes the original signal into a superposition of the number of linearly independent and interpretable subspaces (or components), and then reconstructs the low-ranked approximate of the original signal using the small number of meaningful subspaces. Each of the components represent a unique energy contribution in the signal. The energies of the components vary in unique amplitude patterns over time, such as the slowly varying fluctuations, the coherent oscillations and vibrations, and the random noises (e.g., system noise produced by the optoelectronic instruments and background noise picked up by the sensing fiber). In the decomposed signal, the energies of the slowly varying fluctuations and the coherent oscillations spread over the small individual subsets of subspaces, while the energies of the random noise will be uniformly spread over the whole signal. Therefore,

it is possible to separate the signal of interest from the noise present in the original signal by applying the SVD algorithm.

The original signal of the phase-sensitive OTDR is made by the number of Rayleigh backscattering traces, which provides the spatial and the temporal information of the surrounding environment of the fiber-under-test (FUT). First, the spatial–temporal dataset is arranged into a rectangular matrix to create a 2D image. Assume $A$ is the image matrix of size $m \times n$ ($m \leq n$), where $m$ is the number of Rayleigh backscattering traces and $n$ is the number of sampling points representing the spatial-positions along the FUT in each trace. Thus, there exists a time series, $x_n(t)$, made by the $m$ number of amplitudes for each position. The matrix, $A$, is normalized by dividing all the entries with the spectral norm ($\|A\|_2$). The normalized image matrix, $A$, can be described using the SVD method according to the relation as:

$$A = USV^T \tag{1}$$

$$A = [u_1 \ u_2 \ \cdots \ u_m] \begin{bmatrix} s_1 & 0 & \cdots & 0 & \cdots & 0 \\ 0 & s_2 & \cdots & 0 & \cdots & 0 \\ \vdots & \vdots & \ddots & \vdots & \ddots & \vdots \\ 0 & 0 & \cdots & s_m & \cdots & 0 \end{bmatrix} \begin{bmatrix} v_1^T \\ v_2^T \\ \vdots \\ v_n^T \end{bmatrix} = \sum_{i=1}^{m} u_i s_i v_i^T \tag{2}$$

where $U$ and $V$ are $m \times m$ and $n \times n$ unitary orthogonal matrices, respectively; and $S$ is a $m \times n$ diagonal matrix; rank ($S$) = min ($m$, $n$). The columns of $U$, denoted by $u_i$ of size $m \times 1$, are called left singular vectors; and the rows of $V^T$, denoted by ${v_i}^T$ of size $1 \times n$, are called right singular vectors of matrix $A$. Diagonal entries of matrix $S$ are called the singular values of $A$, and are represented by $s_i$, where $i$ = 1, 2, … , $m$. The left and right singular vectors are the eigenvectors of $AA^{\mathrm{T}}$ and $A^{\mathrm{T}}A$, respectively; and ${s_i}^2$ is the corresponding eigenvalues of A.

The singular values describe information about the importance of their associated subspaces or vectors (left singular and right singular) in the image matrix $A$ in the proposed denoising application for the phase-sensitive OTDR. In the matrix $S$, the singular values are ordered from the highest to the lowest amplitudes, such that $s_1 \geq s_2 \geq \ldots \geq s_j \geq \ldots \geq s_k \geq \ldots \geq s_m \geq 0$. The singular values with higher amplitudes (lowest indexes) represent the singular vectors of the components having high energy-amplitudes (e.g., slowly varying fluctuations, periodic oscillations, and background noises) in the original signal, and the singular values with the lower amplitudes (highest indexes) represent the singular vectors of the components having low energy-amplitudes (such as system noises). From Equation (2), by selecting the appropriate subset of the important singular values having larger amplitudes as well as the associated left and right singular vectors describing only the signal of interest (e.g., intrusion events or vibrations), we can reconstruct the image matrix referred to as, $\tilde{A}$, without significant loss of information. Consequently, we can filter out the undesired energy components from the original signal's data, and could be able to reduce random noise [30]. The reconstructed image matrix, $\tilde{A}$, can be written as:

$$A = \begin{bmatrix} u_j & u_{j+1} & \cdots & u_k \end{bmatrix} \begin{bmatrix} s_j & 0 & \cdots & 0 \\ 0 & s_{j+1} & \cdots & 0 \\ \vdots & \vdots & \ddots & \vdots \\ 0 & 0 & \cdots & s_k \end{bmatrix} \begin{bmatrix} v_j^T \\ v_{j+1}^T \\ \vdots \\ v_k^T \end{bmatrix} = \sum_{i=j}^{k} u_i s_i v_i^T \tag{3}$$

where the size of the reconstructed matrix, $\tilde{A}$, is $m \times n$ (same as $A$), while the sizes of the matrices $U$, $S$, and $V^T$ have been reduced to $m \times r$, $r \times r$, and $r \times n$, respectively; $r = k - j + 1$; $1 < j < k < m$.

Although the SVD denoising method eliminates most of the random noise and the (low-frequency) polarization-dependent interferometric amplitude fluctuations from the original signal, a small amount of background noise is present in the denoised signal. The removal of the low-frequency fluctuations and the background noise is essential for

detection of a weak vibration event. Here, we propose using the weighted singular value decomposition method (WSVD)—a combination of SVD denoising and a weight factor of the position along the sensing fiber. WSVD is expected to enhance the SNR of both the location information and the periodic change in amplitude in the event of applied vibration. The weight factor is a scalar value and is calculated specifically for each position. The weight factor ($w_n$) at specific locations along the sensing fiber can be defined statistically as the energy of its time series, $x_n(t)$, as:

$$w \approx \int |x(t)|^2 dt \tag{4}$$

where $dt$ is the resolution of the time series; $dt$ = pulse duration.

The reconstructed matrix in the Equation (3) can also be written as $\tilde{A} = [\alpha_{ij}]_{m \times n}$ or $A = [\ \alpha_{i1} \quad \alpha_{i2} \quad \alpha_{i3} \quad \cdots \quad \alpha_{in}\ ]$ for $i = 1, 2, \ldots, m$, where $\alpha_{in}$ is the $n$th column vector of size $m \times 1$ for the time series, $x_n(t)$, at the $n$th position along the FUT. Multiplying the time series, $\alpha_{in}$, with its weight factor, $w_n$, further denoises the matrix, $\tilde{A}$. Finally, the weighted reconstructed matrix, $\tilde{A}_w$, can be described as:

$$A_w = [\ w_1\alpha_{i1} \quad w_2\alpha_{i2} \quad w_3\alpha_{i3} \quad \cdots \quad w_n\alpha_{in}\ ] \tag{5}$$

## 3. Experiment and Results

Figure 1a describes the experimental setup of the phase-sensitive OTDR for vibration sensing [11,12]. A continuous-wave (cw) light launched from a highly coherent laser source (λ ~1554.2 nm) with ultra-narrow line width (~6 kHz) was modulated into the light pulses using the semiconductor amplifier (SOA) functioning as a switch. An isolator was installed between the laser and SOA to protect the laser from unwanted light reflections from the SOA, and optical features of the light pulse were optimized using a polarization controller (PC). Using an erbium-doped fiber amplifier (EDFA), the optical light pulse was amplified and the undesired ASE light was filtered out. Subsequently, a band-pass filter (BPF), made by an optical circulator and a fiber Bragg grating (FBG) (λ ~1554 nm, Δλ ~0.32 nm, reflectivity ~30 dB) filtered out the undesired ASE light. Before entering into FUT, the input optical power should be controlled to be ≤23 dBm using a variable optical attenuator (VOA) to evade the possible nonlinear effects in the silica optical fiber. Then, the optical pulse was fed into the FUT and the coherent Rayleigh backscattering reflection was detected at the photodiode (PD) via the optical fiber circulator. Finally, the analog electrical signal was digitized using a high-speed data acquisition (DAQ) card, and analyzed by the computer.

Figure 1b,c illustrates the vibration actuation setups, which are made by the mechanical actuator and the sound-speaker, respectively. A fiber loop of length 9 m was attached firmly on the setups using a removable tape at the particular position of ~1245 m of the FUT. The vibration setups were driven by a function generator, whose frequency can be controlled from several Hz to kHz range. In the experiment, we set the pulse width to 90 ns and the pulse repetition rate to 10 kHz (pulse duration = 100 μs), which means that the Φ-OTDR had a spatial resolution of 9 m and a detection range of 10 km. Using a DAQ module, we acquired 610 raw traces of the RBS signal using the setup given in Figure 1b, and 800 raw traces of the RBS signal using the setup given in Figure 1c; thus, the total data-acquisition times were 61 and 80 ms, respectively. During data acquisition, the sampling speed of the DAQ was 50.2 MS/s.

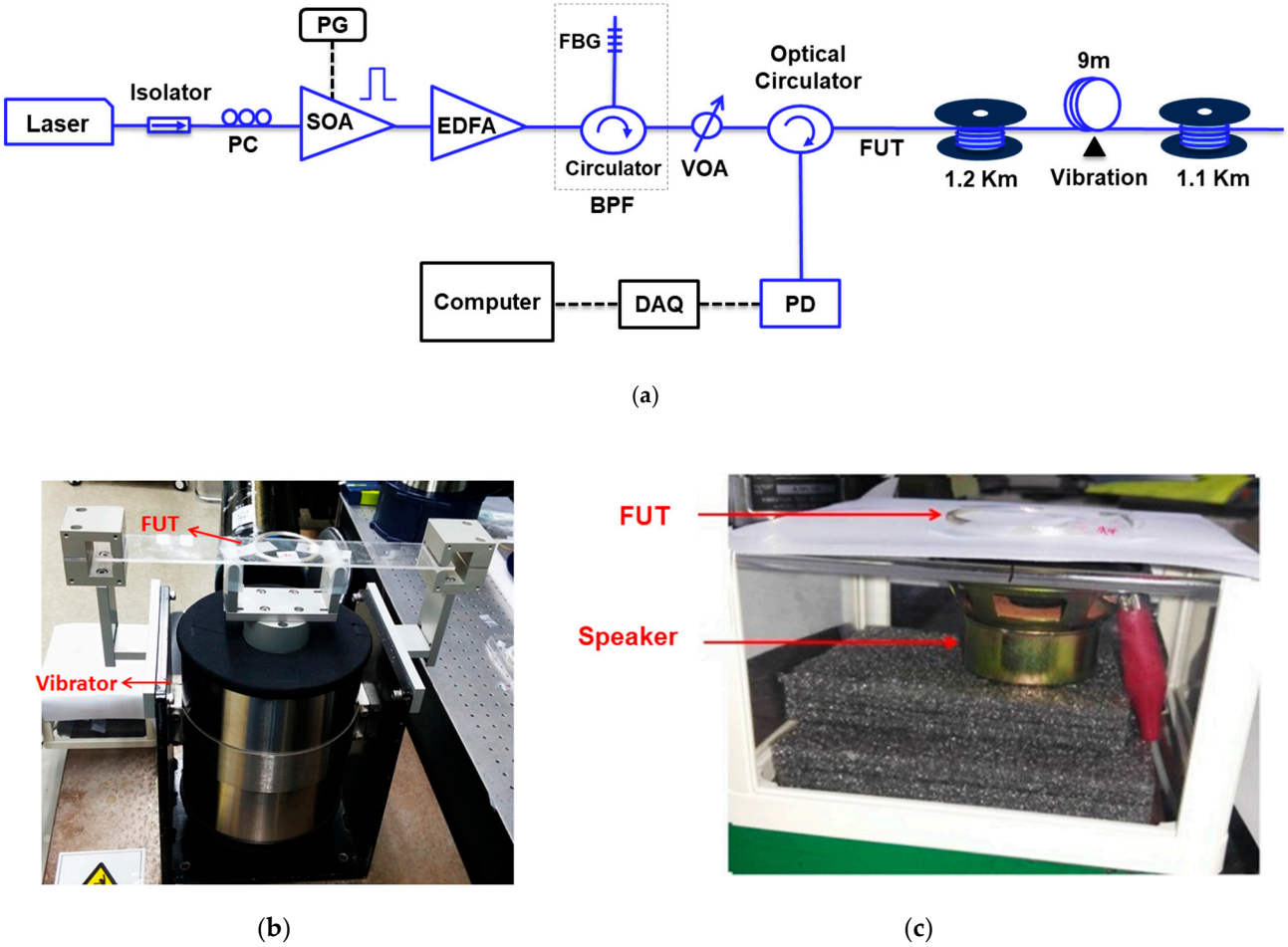


**Figure 1.** (**a**) Experimental setup of the phase-sensitive optical time-domain reflectometer (OTDR)-based vibration sensor. Above are the images showing the vibration setup in order to induce: (**b**) physical perturbation using a mechanical actuator, and (**c**) acoustic perturbation using a sound-speaker on the 9 m fiber loop placed at specific position of the fiber-under-test (FUT).

Figure 2a shows the plot of the 610 consecutive raw Rayleigh backscattering traces along the length of the FUT. The plot contains the coherent amplitude modulation at specific positions caused by the fiber loop when subjected to a weak vibration event of 102 Hz using the mechanical actuator shown in Figure 1b. The Rayleigh backscattering traces were created by the coherent superposition of the light from multiple scattering centers along the FUT within the duration of optical pulse. The raw Rayleigh backscattering traces show the overall amplitude fluctuation. The fluctuation could be due to phase noise of the laser, random polarization causing partial interferometric issue, or background and electrical noises (thermal noise and shot noise). Moreover, amplitude-fading also exists in the signal after 1500 m. This is thought to be due to the input power of pulse light, which is slightly larger than the nonlinearity limit of the single-mode fiber used as the FUT. Thus, it was difficult to determine the location information and the frequency of the vibration event in the backscattering traces, which are badly affected by the random noises. Figure 2b shows a transformation of the amplitude data of the 610 raw Rayleigh backscattering traces (given in Figure 2a) to a density plot (gray image); the horizontal axis shows the spatial information and the vertical axis shows the temporal information of the dataset. The weak periodic change in the amplitude, which can be seen in the inset at the FUT location of 1245 m, was caused by the external vibration event (102 Hz). Nevertheless, the presence of random noises in the raw backscattering traces of the phase-sensitive OTDR made it difficult to truly detect the vibration event (location information and vibration

frequency) and could lead to false alarms in real-life applications. Therefore, we present the WSVD method to denoise the backscattering traces to extract the accurate information of the vibration event.

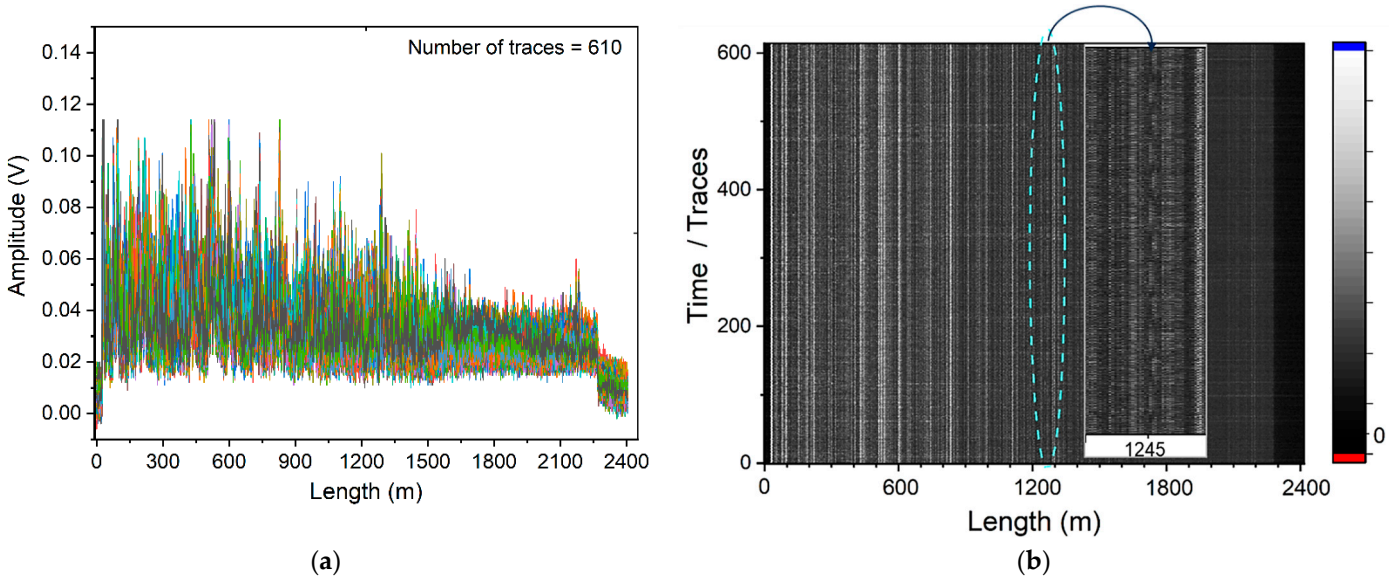


**Figure 2.** Consecutive raw traces of the Rayleigh backscattering reflections obtained from the phase-OTDR. The dataset is shown as (**a**) a location information plot and (**b**) a density plot.

We performed the WSVD on the raw backscattering traces assembled in the form of image matrix $A$, according to the theory described in Equations (1)–(5). In the decomposition of the image matrix as given in Equation (2), we obtained the $m$ number of singular values and the associated left and right singular vectors from the $m$ number of RBS traces. Figure 3 describes the normalized magnitudes of singular values as a function of the number of RBS traces. In the figure, the magnitudes are normalized, and the first normalized singular value (=1) is omitted. Our analyses showed that in the original signal, the first set of largest 30 singular values having the magnitudes in the range of 1–0.015 represent the slowly varying components having energies greater than those of the vibration event. The next set of 145 singular values having the magnitudes in the range of 0.015–0.0065 represents the energies of the vibration event. The rest of the singular values having magnitudes lower than the 0.0065 represents the energies of the noise components. Importantly, even though the number ($m$) of RBS traces in the dataset changed from 610 to 310 in a step of 100, the magnitudes of their $m$ number of singular values varied slightly, and followed nearly similar decreasing trends. The serials of the set containing the singular values of interest, due to slight change in the associated magnitudes with the change in the $m$, could be slightly shifted. Thus, it is expected that there will be no considerable effect of changing the number of RBS traces on the amplitudes of the associated singular vectors, and hence the SNR of the location information will not be significantly changed. According to the Nyquist theorem, the number of backscattering traces in the original signal must be at least twice the frequency of the applied vibration to be measured accurately. For $m$ = 610 traces (and so 610 singular values), we carefully chose the energy components of interest corresponding to the set of singular values in the magnitude range of 0.015–0.0065, and obtained the reconstructed image matrix according to Equation (3). In the said range, there are about 145 singular values from the serial number 30 to 175, which makes about 4–25% of the total 610 values. This means that by selecting the 4–25% of the associated energy components to make matrix $\tilde{A}$, we were able to filter out the slowly varying amplitude fluctuation and substantial residual noise having energies higher or lower than those of the applied vibration from the original signal. Thereafter, to increase the SNR of the vibration event and to preserve the frequency of the event, the weight factors for positions were

included in the reconstructed image matrix $\tilde{A}$, following Equation (5). This completed the process of denoising the original signal using WSVD, and produced *a* denoised signal in the form of weighted image matrix $\tilde{A}_w$.

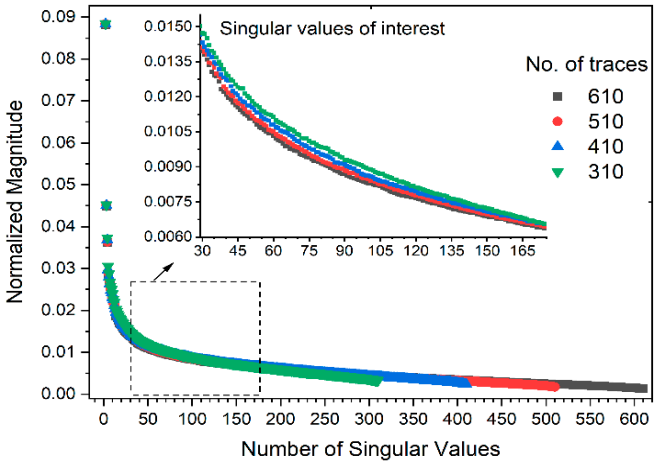


**Figure 3.** Singular value distribution of the original spatial-temporal dataset of the phase-sensitive OTDR.

Figure 4a,b presents the location information and the periodic change in amplitude caused by the weak vibration event of 102 Hz, respectively, using the WSVD-based denoising method. It can be seen that a weak vibration event was clearly detected with a dominant peak at the location of ~1245 m, whose amplitude variation shown in Figure 4b is essential for the measurement of vibration frequency.

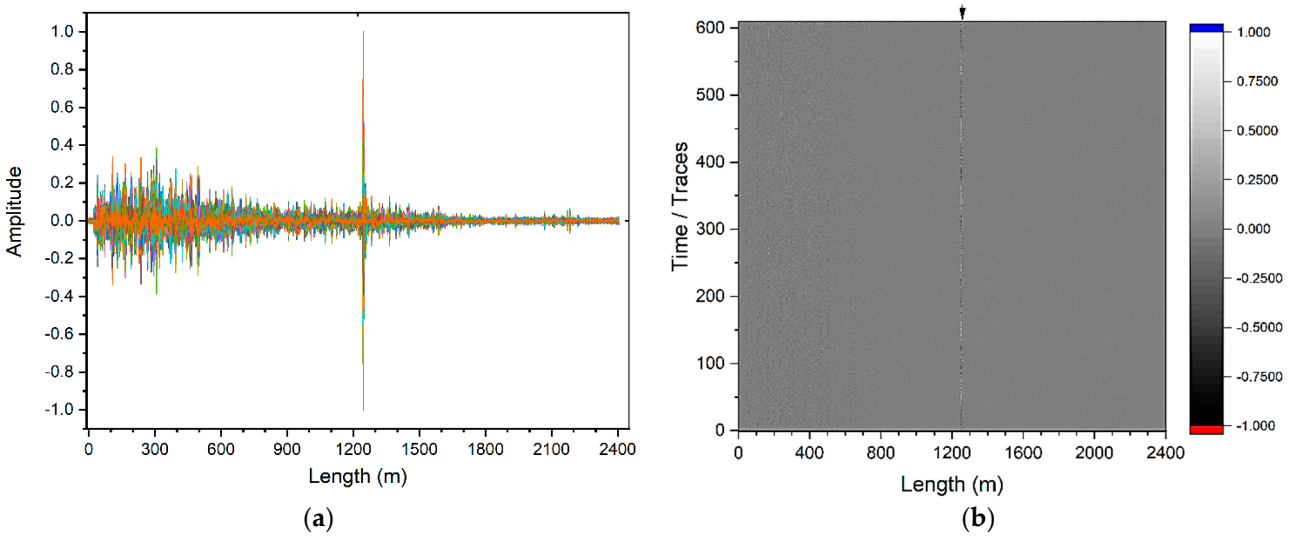


**Figure 4.** Denoised traces of the Rayleigh backscattering (RBS) reflections obtained after applying the weighted singular value decomposition (WSVD) method for detection of the vibration event of 102 Hz: (**a**) location plot for event detection, and (**b**) density plot for frequency measurement.

Figure 5a,b presents the square of the location information for detection of the vibration event of 102 Hz obtained by the moving differential method [6] and the WSVD method, respectively. The performance of the two methods can be estimated using the SNR of the event detection. For a vibration event, if $V_s$ is the voltage of the signal peak and $V_n$ is

the voltage of the background noise, then the SNR of the location information is defined as [19]:

$$SNR = 10log_{10}\left(\frac{V_s}{V_n}\right) \quad (6)$$

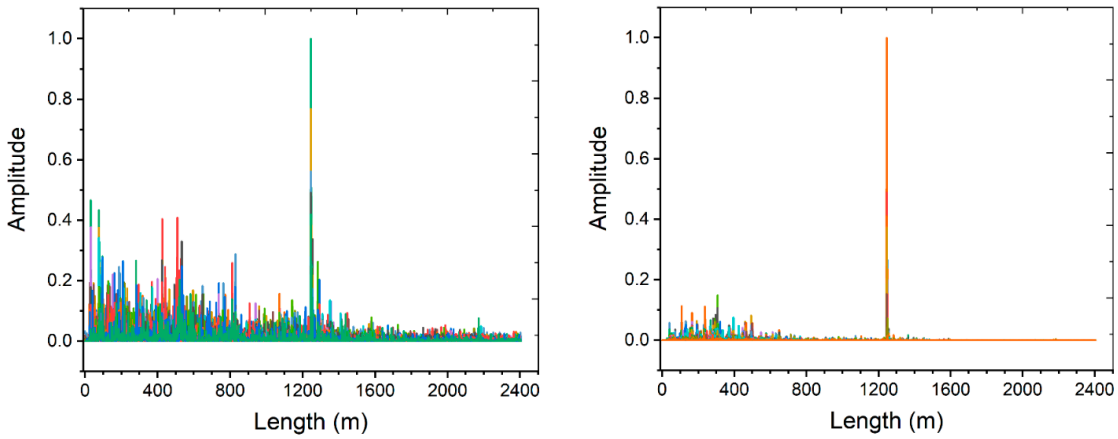


**Figure 5.** Denoised traces of the Rayleigh backscattering reflections, showing the detection of the physical event of 102 Hz, are obtained after applying (**a**) the moving differential method and (**b**) the WSVD.

Here, the voltage amplitude of the denoised backscattering traces is normalized and scaled in the range of 0–1. In Figure 5a, the amplitudes of signal and noise are found to be 1 and 0.275 using the moving differential method, respectively, so the SNR is equal to 5.6 dB. In Figure 5b, the SNR is 10.7 dB by applying the WSVD method. It is evident that the SNR of location information is significantly increased by the application of the proposed WSVD method on the original signal.

Figure 6a describes a density plot made by the 800 raw Rayleigh backscattering traces comprising an acoustic event of 525 Hz, which was generated using a sound speaker, as given in Figure 1c. Again, the acoustic signal was very weak and difficult to be observed using our vision in the plot. However, when the raw traces were processed using the WSVD method, as can be seen in Figure 6b, a unique periodic change in voltage amplitude compared with the density plot of 102 Hz (see Figure 4b) was found at the position of 1245 m of the sensing fiber.

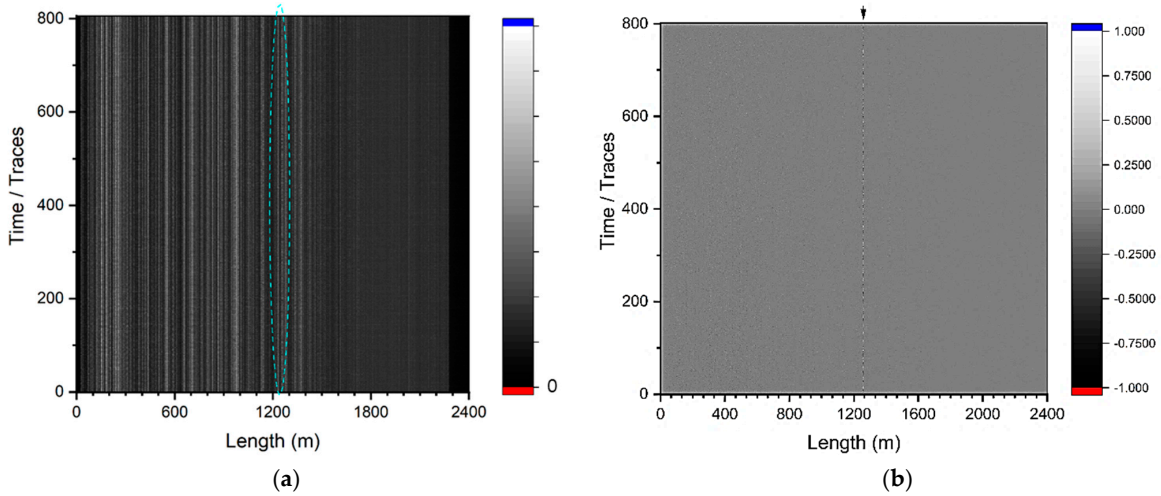


**Figure 6.** Traces of the Rayleigh backscattering reflections, which consist of an acoustic event of 525 Hz, are shown in the density plot: (**a**) before and (**b**) after denoising using the WSVD.

The location information yielded after processing by different methods is illustrated in Figure 7. In a similar manner, the noise was removed and the SNR of the vibration event was estimated using two different methods. In Figure 7a, the SNR of the vibration event of 525 Hz is detected to be 5.23 dB by employing the moving differential method, whereas it is obtained to be 12.2 dB by employing the WSVD as shown in Figure 7b.

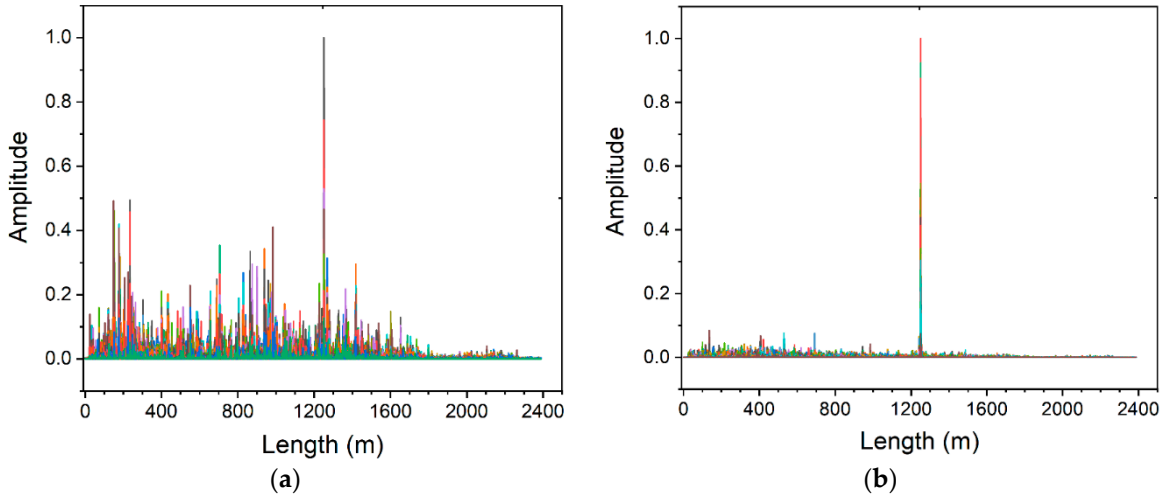


**Figure 7.** Denoised traces of the Rayleigh backscattering reflections, showing the detection of an acoustic event of 525 Hz, obtained after applying (**a**) the moving differential method and (**b**) the WSVD.

Figure 8 describes the quantitative comparison between the SNR of the vibration event processed by the two different methods. Clearly, the raw backscattering traces processed by the WSVD method show a remarkable ~6.5 dB improvement in the SNR of the vibration events of 102 and 525 Hz.

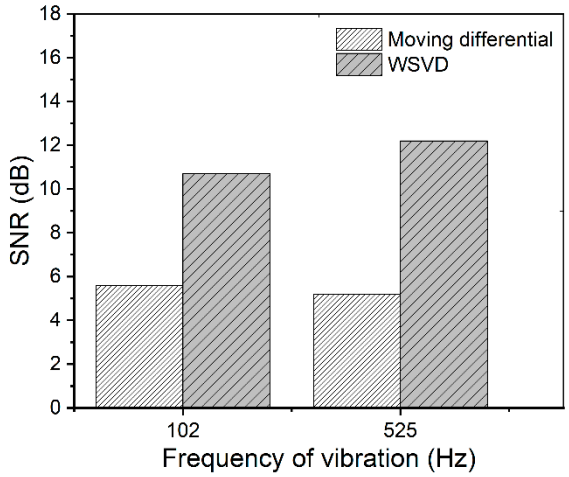


**Figure 8.** Comparison of the signal-to-noise ratio (SNR) of the location information obtained by using the two signal-denoising methods.

To confirm the vibration sensing, Fourier transform was applied on the denoised temporal data at the location of vibration event. Figure 9 shows the normalized power spectra for the vibration events of 102 and 525 Hz at the ~1245 m location. The vibration frequencies of the two events were measured with an error <0.5 Hz.

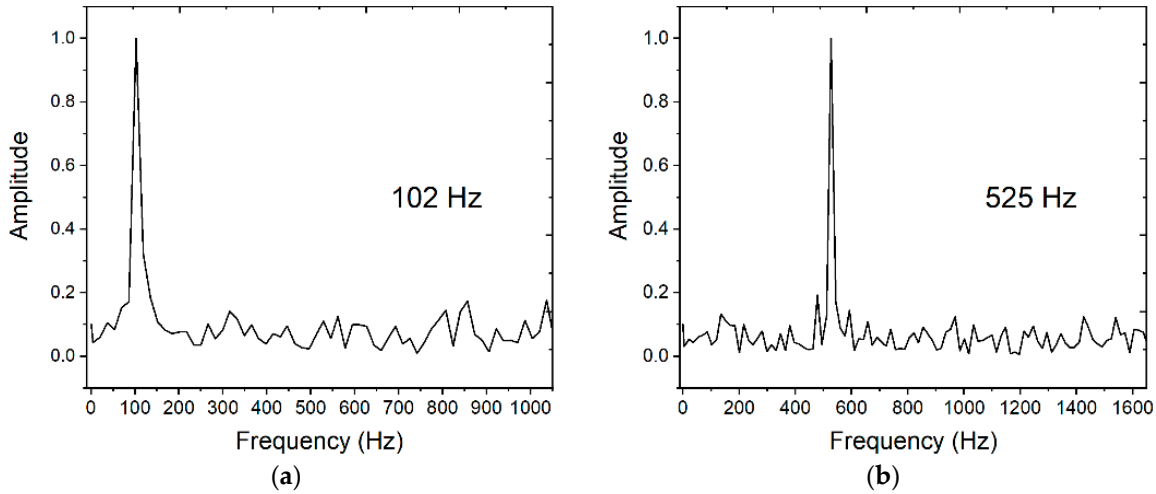


**Figure 9.** Power spectrum of the denoised temporal data is obtained at the location of the vibration event having a frequency of (**a**) 102 and (**b**) 525 Hz.

## 4. Conclusions

In summary, we proposed and demonstrated a novel denoising technique that uses the weighted singular value decomposition to improve the detection performance of the phase-sensitive OTDR-based distributed vibration sensor. The multiple time traces along the length of FUT, which form the original signal, were arranged to create a 2D image matrix. The application of the proposed WSVD method decomposes the image matrix into the superposition of numbers of independent and interpretable subspaces with unique singular values. By selecting the suitable set of subspaces in the reconstruction, the WSVD method removes the low-frequency polarization-dependent fluctuation and background noise from the original signal. The weight factor along the length of the fiber further eliminates the random noises, thus efficiently denoising the original signal. In the event of applied vibration, the location information and the frequency of vibration are successfully retrieved along a 2.4 km single mode fiber with a 9 m spatial resolution. The SNR of the location information was found to be 10.7 dB for the physical vibration of 102 Hz, and 12.2 dB for an acoustic vibration of 525 Hz. Compared to the conventional method, the SNR of the vibration event obtained after the proposed denoising method exhibited an increase in the range of 6–7 dB, which confirmed the usefulness of the denoising capability of this new approach of WSVD for a truly-distributed vibration sensor based on the phase-sensitive OTDR.

**Author Contributions:** Conceptualization, K.N.; methodology, K.N.; software, K.N.; validation, B.H.K. and I.-B.K.; formal analysis, K.N.; investigation, K.N.; resources, B.H.K. and I.-B.K.; data curation, K.N.; writing—original draft preparation, K.N.; writing—review and editing, D.-J.Y. and I.-B.K.; visualization, K.N. and D.-J.Y.; supervision, B.H.K. and I.-B.K.; project administration, B.H.K. and I.-B.K.; funding acquisition, B.H.K. and I.-B.K. All authors have read and agreed to the published version of the manuscript.

**Funding:** This research work was supported by GIST Research Institute (GRI) APRI under a grant funded by GIST in 2021, and by the Korea Ministry of Environment (MOE) as a Service Program for Demand-Responsive Water Supply (127587).

**Institutional Review Board Statement:** Not applicable.

**Informed Consent Statement:** Not applicable.

**Data Availability Statement:** Data is contained within the article.

**Conflicts of Interest:** The authors declare no conflict of interest.

## References


1. Shao, L.-Y.; Liu, S.; Bandyopadhyay, S.; Yu, F.; Xu, W.; Wang, C.; Li, H.; Vai, M.I.; Du, L.; Zhang, J. Data-Driven Distributed Optical Vibration Sensors: A Review. *IEEE Sens. J.* **2019**, *20*, 6224–6239. [CrossRef]
2. Rogers, A. Distributed optical fiber sensing. *Meas. Sci. Technol.* **1999**, *10*, R75–R99. [CrossRef]
3. Muanenda, Y. Recent advances in distributed acoustic sensing based on phase-sensitive optical time domain reflectometry. *J. Sens.* **2018**, *2018*, 3897873. [CrossRef]
4. Ren, M.Q.; Lu, P.; Chen, L.; Bao, X.Y. Study of F-OTDR stability for dynamic strain measurement in piezoelectric vibration. *Photonic Sens.* **2016**, *6*, 199–208. [CrossRef]
5. Zhou, L.; Wang, F.; Wang, X.; Pan, Y.; Sun, Z.; Hua, J.; Zhang, X. Distributed Strain and Vibration Sensing System Based on Phase-Sensitive OTDR. *IEEE Photon Technol. Lett.* **2015**, *27*, 1884–1887. [CrossRef]
6. Lu, Y.; Zhu, T.; Chen, L.; Bao, X. Distributed Vibration Sensor Based on Coherent Detection of Phase-OTDR. *J. Light. Technol.* **2010**, *28*, 3243–3249. [CrossRef]
7. Koyamada, Y.; Imahama, M.; Kubota, K.; Hogari, K. Fiber-Optic Distributed Strain and Temperature Sensing with Very High Measurand Resolution Over Long Range Using Coherent OTDR. *J. Light. Technol.* **2009**, *27*, 1142–1146. [CrossRef]
8. Wang, Z.; Pan, Z.; Fang, Z.; Ye, Q.; Lu, B.; Cai, H.; Qu, R. Ultra-broadband phase-sensitive optical time-domain reflectometry with a temporally sequenced multi-frequency source. *Opt. Lett.* **2015**, *40*, 5192–5195. [CrossRef]
9. Wang, C.; Wang, C.; Shang, Y.; Liu, X.; Peng, G. Distributed acoustic mapping based on interferometry of phase optical time-domain reflectometry. *Opt. Commun.* **2015**, *346*, 172–177. [CrossRef]
10. Franciscangelis, C.; Margulis, W.; Kjellberg, L.; Soderquist, I.; Fruett, F. Real-time distributed fiber microphone based on phase-OTDR. *Opt. Express* **2016**, *24*, 29597. [CrossRef]
11. Peng, F.; Duan, N.; Rao, Y.-J.; Li, J. Real-Time Position and Speed Monitoring of Trains Using Phase-Sensitive OTDR. *IEEE Photon-Technol. Lett.* **2014**, *26*, 2055–2057. [CrossRef]
12. Juarez, J.; Maier, E.; Choi, K.N.; Taylor, H. Distributed fiber-optic intrusion sensor system. *J. Light. Technol.* **2005**, *23*, 2081–2087. [CrossRef]
13. Wu, H.; Wang, Z.; Peng, F.; Peng, Z.; Li, X.; Wu, Y.; Rao, Y. Field Test of a Fully Distributed Fiber Optic Intrusion Detection System for Long-Distance Security Monitoring of National Borderline. In Proceedings of the OFS2014 23rd International Conference on Optical Fiber Sensors, Santander, Spain, 2–6 June 2014.
14. Martins, H.F.; Martin-Lopez, S.; Corredera, P.; Salgado, P.; Frazão, O.; González-Herráez, M. Modulation instability-induced fading in phase-sensitive optical time-domain reflectometry. *Opt. Lett.* **2013**, *38*, 872–874. [CrossRef] [PubMed]
15. Wang, Z.N.; Li, J.; Fan, M.Q.; Zhang, L.; Peng, F.; Wu, H.; Zeng, J.J.; Zhou, Y.; Rao, Y.J. Phase-sensitive optical time-domain reflectometry with Brillouin amplification. *Opt. Lett.* **2014**, *39*, 4313–4316. [CrossRef] [PubMed]
16. Martins, H.F.; Martin-Lopez, S.; Corredera, P.; Filograno, M.L.; Frazao, O.; Gonzalez-Herraez, M. Phase-sensitive Optical Time Domain Reflectometer Assisted by First-order Raman Amplification for Distributed Vibration Sensing Over >100 km. *J. Light. Technol.* **2014**, *32*, 1510–1518. [CrossRef]
17. Wang, Z.N.; Zeng, J.J.; Li, J.; Fan, M.Q.; Wu, H.; Peng, F.; Zhang, L.; Zhou, Y.; Rao, Y.J. Ultra-long phase-sensitive OTDR with hybrid distributed amplification. *Opt. Lett.* **2014**, *39*, 5866–5869. [CrossRef] [PubMed]
18. Ibrahim, A.D.A.; Lin, S.; Xiong, J.; Jiang, J.; Fu, Y.; Wang, Z. Integrated principal component analysis denoising technique for phase-sensitive optical time domain reflectometry vibration detection. *Appl. Opt.* **2020**, *59*, 669–675. [CrossRef]
19. Qin, Z.; Chen, H.; Chang, J. Detection Performance Improvement of Distributed Vibration Sensor Based on Curvelet Denoising Method. *Sensors* **2017**, *17*, 1380. [CrossRef]
20. Qin, Z.; Chen, H.; Chang, J. Signal-to-Noise Ratio Enhancement Based on Empirical Mode Decomposition in Phase-Sensitive Optical Time Domain Reflectometry Systems. *Sensors* **2017**, *17*, 1870. [CrossRef]
21. Qin, Z.; Chen, L.; Bao, X. Wavelet Denoising Method for Improving Detection Performance of Distributed Vibration Sensor. *IEEE Photon Technol. Lett.* **2012**, *24*, 542–544. [CrossRef]
22. He, M.; Feng, L.; Zhao, D. A method to enhance SNR based on CEEMDAN and the interval thresholding in Φ_OTDR sys-tems. *Appl. Phys. B* **2020**, *126*, 97. [CrossRef]
23. Li, Q.; Zhang, C.; Li, L.; Zhong, X. Signal-to-noise ratio enhancement of phase-sensitive optical time-domain reflectometry based on power spectrum analysis. *Opt. Eng.* **2014**, *53*, 26106. [CrossRef]
24. Zhu, T.; Xiao, X.; He, Q.; Diao, D. Enhancement of SNR and Spatial Resolution in $\varphi$-OTDR System by Using Two-Dimensional Edge Detection Method. *J. Light. Technol.* **2013**, *31*, 2851–2856. [CrossRef]
25. He, H.; Shao, L.; Li, H.; Pan, W.; Luo, B.; Zou, X.; Yan, L. SNR Enhancement in Phase-Sensitive OTDR with Adaptive 2-D Bilateral Filtering Algorithm. *IEEE Photon J.* **2017**, *9*, 1–10. [CrossRef]
26. Chen, W.; Duan, W. Computational Aspects of Mathematical Models in Image Compression. Master's Thesis, Chalmers University of Technology, Gothenburg, Sweden, 2009.
27. Yaacoub, F.; Abche, A.; Karam, E.; Hamam, Y. MRI Reconstruction Using SVD in the Least Square Sense. In Proceedings of the 21st IEEE International Symposium on Computer-Based Medical Systems, Washington, DC, USA, 17–19 June 2008; pp. 47–49.
28. Yang, W.; Hong, J.-Y.; Kim, J.-Y.; Paik, S.-H.; Lee, S.H.; Park, J.-S.; Lee, G.; Kim, B.M.; Jung, Y.-J. A Novel Singular Value De-composition-Based Denoising Method in 4-Dimensional Computed Tomography of the Brain in Stroke Patients with Statistical Evaluation. *Sensors* **2020**, *20*, 3063. [CrossRef] [PubMed]

29. Guo, Q.; Zhang, C.; Zhang, Y.; Liu, H. An Efficient SVD-Based Method for Image Denoising. *IEEE Trans. Circuits Syst. Video Technol.* **2015**, *26*, 868–880. [CrossRef]
30. Lyra-Leite, D.M.; Da Costa, J.P.C.L.; De Carvalho, J.L.A. Improved MRI reconstruction and denoising using SVD-based low-rank approximation. In Proceedings of the 2012 Workshop on Engineering Applications, Bogota, Colombia, 2–4 May 2012; IEEE: Bogota, Colombia, 2012; pp. 1–6.